

Studies of dual-harmonic acceleration at CSNS-II *

CHEN Jin-Fang(陈锦芳)^{1,2} TANG Jing-Yu(唐靖宇)^{1:1)}

¹ Institute of High Energy Physics, CAS, Beijing 100049, China

² Graduate University of Chinese Academy of Sciences, CAS, Beijing 100049, China

Abstract The Rapid Cycling Synchrotron (RCS) of the China Spallation Neutron Source (CSNS) complex is designed to provide 1.56×10^{13} protons per pulse (ppp) during the initial stage, and it is upgradeable to 3.12×10^{13} ppp during the second stage and 6.24×10^{13} ppp during the ultimate stage. The high beam intensity in the RCS requires alleviation of space charge effects to reduce beam losses, which is key in such high beam power accelerators. With higher intensities in the upgrading phases, a dual-harmonic RF system is planned to produce flat-topped bunches that are useful to reduce the space charge effects. We have studied different schemes to apply the dual-harmonic acceleration in CSNS-II, and have calculated the main parameters of the RF systems, which are presented in this paper.

Key words space charge effects, bunching factor, dual-harmonic RF acceleration

PACS 29.25.Dz, 29.20.dk

1 Introduction

The China Spallation Neutron Source (CSNS) [1, 2] is a short-pulse accelerator facility mainly consisting of an H^- linac and a proton rapid cycling synchrotron (RCS). As shown in Table 1, the accelerator is designed to accelerate proton beams to 1.6 GeV in kinetic energy at a repetition rate of 25 Hz. It delivers

a proton beam of 100 kW in beam power in the first phase with an upgrading capability to 200 kW in the second phase by increasing the linac output energy from 80 MeV to 130 MeV, and increasing the average beam intensity at the same time. Meanwhile, the accumulated protons in the RCS are increased from 1.56×10^{13} to 3.12×10^{13} . The main parameters for the third upgrading phase are also listed in the table.

Table 1. Some basic parameters of the CSNS RCS.

project phase	I	II	III
ring circumference/m	228	228	228
curvature of bending magnet/m	8.1487	8.1487	8.1487
beam power/kW	100	200	500
No. of RF cavities	8 ($h=2$)	8 ($h=2$)+3 ($h=4$)	8 ($h=2$)+3($h=4$)
injection energy/MeV	80	130	250
extraction energy /GeV	1.60	1.60	1.60
protons per pulse/ 10^{13}	1.56	3.12	6.24
repetition rate/Hz	25	25	25

The 2nd higher harmonic RF system ($h=4$, abbr. as H4 cavities) will be added to the fundamental one ($h=2$, abbr. as H2 cavities) in the RCS for CSNS-II. The studies concerning the longitudinal motion with the dual-harmonic RF system are presented in this paper. The situation in CSNS-III is similar, but

it will not be discussed in this paper. Compared with CSNS-I, the number of accumulated protons and the extracted beam power are doubled at CSNS-II. Generally speaking, higher beam intensity means stronger space charge effects, which may cause severe beam loss. To alleviate the space charge effects, we

Received 19 January 2010

* Supported by National Natural Science Foundation of China (10775153)

1) Corresponding author: tangjy@ihep.ac.cn

©2010 Chinese Physical Society and the Institute of High Energy Physics of the Chinese Academy of Sciences and the Institute of Modern Physics of the Chinese Academy of Sciences and IOP Publishing Ltd

add some H4 cavities along with higher injection energy at CSNS-II. The layout of the RCS is shown in Fig. 1.

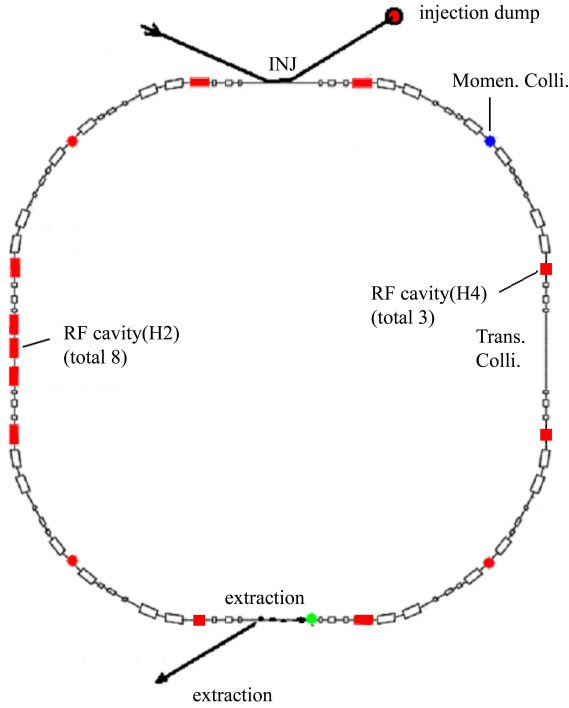


Fig. 1. Functional layout of the RCS with eight H2 cavities and three H4 cavities.

There have been other proton synchrotrons in the world applying dual-harmonic RF system to improve the control on beam bunch shape; for example, the PS booster at CERN [3], the AGS booster at BNL [4] and the RCS at ANL [5]. At ISIS, the 2nd higher harmonic cavities were installed and the initial operation shows that the beam loss rate becomes dramatically smaller [6]. At J-PARC, a dual-harmonic RF is used at a lower energy range to improve the bunching factor [7].

Similar to ISIS and J-PARC, at CSNS-II, we also plan to use a dual-harmonic RF to obtain flat-topped bunches and to control the beam loss rate.

The theory of dual-harmonic acceleration is briefly described in Section 2. The calculation results with the CSNS-II parameters are presented in Section 3.

2 Dual-harmonic acceleration and Laslett tune shift

Beam bunch shape is determined by the RF bucket after the beam capture in the longitudinal phase plane, while the bucket shape depends on the RF voltage waveform. By adjusting the waveform

by adding a higher harmonic RF component, a long flat-topped bunch can be created. A lower peak line charge density of the bunch means a larger bunching factor and a smaller Laslett tune shift, which is required to reduce the beam losses.

2.1 RF acceleration voltage waveforms

When the applied RF voltage is sinusoidal and the dual-harmonic RF voltage is a combination of the fundamental harmonic h and the second higher harmonic $2h$ components, the total voltage (as shown in Fig. 2) can be written in the form

$$V(\phi) = V_1 [\sin(h\omega t) - \delta \sin(2h\omega t + \theta)], \quad (1)$$

where V_1 is the amplitude of the harmonic h , δV_1 is the amplitude of the harmonic $2h$, ω is the mean angular cycling frequency of the beam and θ is the relative phase between the two RF systems with different harmonics.

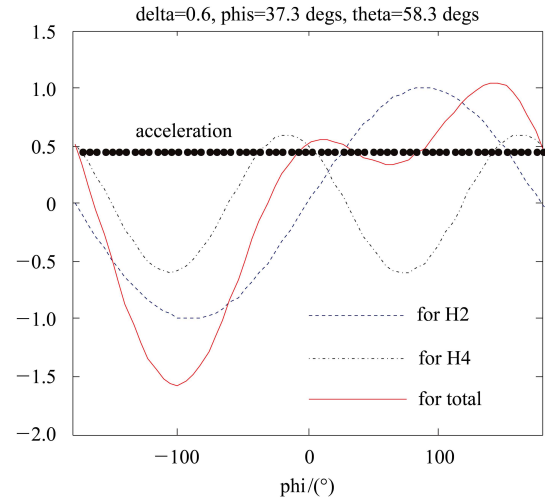


Fig. 2. Voltage waveforms of a dual-harmonic RF system (in unit of H2 voltage).

For a synchronous particle, the acceleration voltage has the following relation to the ramping rate of the bending field,

$$V_0 = 2\pi R \rho \dot{B} = V_1 [\sin \phi_s - \delta \sin(2\phi_s + \theta)], \quad (2)$$

where R is the mean radius of the ring, and ρB is the product of the curvature radius and the magnetic field in a ring dipole.

For convenience, we mark $\hat{A} = 2\pi R \rho \dot{B} / V_1$ (shown as the dashed curve in Fig. 2). The value of \hat{A} depends on \dot{B} / V_1 . When $\delta = 0$, assuming $\hat{A} < 1$, there are two solutions to Eq. (2) in the range of $[-\pi, \pi]$. When $\delta \neq 0$, if the voltage is high enough to have $\hat{A} < 0.5$, in most cases with the condition of $\delta \leq 0.6$ and $\theta \leq 0$, there are four solutions to Eq. (2), and

this can increase the bucket size or the stable region in the longitudinal phase space [8]. However, if \hat{A} is increased above 0.5, the ranges of acceptable δ and θ will diminish. When $\hat{A} > 0.7$, it will be not possible to find out a combination of δ and θ to give four solutions. Therefore, the relevant voltages should not be too low to maintain a reasonable \hat{A} .

For example, the magnet field ramps up and down by following a DC-biased sinusoidal curve in CSNS: $B(t) = B_0 - B_1 \cos(2\pi ft)$, where $B_0 = 0.5961$ T, $B_1 = 0.3839$ T, $f = 25$ Hz. At the moment of 2 ms (zero moment denotes the lowest field), $\hat{A}_{\max} V_{1\max} \geq 2\pi\rho R \dot{B}|_{\max} = 34$ kV, then $V_{1\max}$ reaches 48.7 kV at

$$V_t(\phi) = \begin{cases} V(\phi) - 2\pi h^2 I_b \text{Im}\{Z_e/n\} \frac{V(\phi) - V_0}{u(\phi_1, \phi_2)}, & \phi_1 < \phi < \phi_2 \\ V(\phi), & \text{elsewhere} \end{cases}, \quad (3)$$

where $Z_e/n = -j[(g_0 Z_0 / 2\beta\gamma^2) - w_0 L]$ is the space charge impedance, and the second term is the inductance of the vacuum chamber wall. For synchrotrons of low energy, the longitudinal space charge force is far stronger than the inductive wall force, thus the latter may be ignored. I_b is the mean current per bunch. $u(\phi_1, \phi_2) = -V_1 F(\phi_1, \phi_2)$, where ϕ_1 and ϕ_2 are the phase extremity values for the full phase stable region and $F(\phi_1, \phi_2)$ is a function defined in Eq. (9).

2.2 Bucket area of a dual-harmonic RF system

The longitudinal beam loss in the ring primarily happens in the RF capture stage and the initial acceleration stage when the energy is still low. Ideally, the RF bucket is large enough to encase all particles to avoid the longitudinal beam loss. However, a large bucket usually means a large RF voltage that is equivalent to the higher cost of the RF system. At CSNS, the beam is injected by filling into the bucket with a chopped beam and the off-momentum method. Since the bunch area is almost constant during the acceleration, it is important to keep the bucket area undiminished, namely, the bucket size is constant or increasing during acceleration. Due to the emittance blow-up, some particles can still escape from the bounding of the RF focusing and get lost. From the compromise between the RF voltage and the beam loss, we can design the bucket size as constant in the early accelerating stage but somewhat increased later when the RF voltage is less exigent.

In the longitudinal phase space expressed by $(\phi, \Delta E/h\omega_0)$, the bucket per bunch is given by

least for $\hat{A}_{\max} \leq 0.7$.

The longitudinal distribution of the beam is formed by a longitudinal painting process where different techniques can be used to fill the injection beam in the longitudinal phase plane. At CSNS, the off-moment method is used [9]. When the space charge effects are taken into account, the longitudinal charge density distribution will be an elliptical 2-D Hofmann-Pedersen distribution [10]. The longitudinal space charge force from the inductive vacuum wall is proportional to the external containing forces. The total voltage of the combined RF voltage and the space-charge voltage is given by

$$A = 8R \sqrt{\frac{2eV_1(1-\eta_{sc})E_0\gamma\alpha^2}{h^3 c^2 \pi \eta}}, \quad (4)$$

where e is the unit of electronic charge. The space charge factor η_{sc} is expressed by

$$\eta_{sc} = \frac{2\pi h^2 I_b \text{Im}\{Z_e/n\}}{u(\phi_1, \phi_2)}, \quad (5)$$

where E_0 is the rest energy, γ is the relativity energy factor, c is the velocity of light, η is the phase slippage factor ($\eta = \gamma_t^{-2} - \gamma^{-2}$), and the factor α [11] is the ratio of the bucket areas between a running bucket ($\phi_s \neq 0$) and a stationary bucket ($\phi_s = 0$),

$$\alpha(\phi) = \frac{1}{4\sqrt{2}} \int_{\phi_1}^{\phi_2} \left\{ -\frac{|\eta|}{\eta} \left[\cos\phi - \cos\phi_2 \right. \right. \\ \left. \left. + (\phi - \phi_2) \sin\phi_s - \frac{\delta}{2} (\cos(2\phi + \theta) - \cos(2\phi_2 + \theta)) \right. \right. \\ \left. \left. - \delta(\phi - \phi_2) \sin(2\phi_2 + \theta) \right] \right\}^{1/2} d\phi. \quad (6)$$

2.3 Laslett tune shift due to the space charge

The transverse defocusing generated by the space charge force will change the theoretical lattice functions and the betatron tunes. The average tune shift and the tune spread or tune footprint may cause a part of the beam or even the whole beam to cross through some resonant lines. Although the low-order structure resonances that are very dangerous are usually avoided in the lattice design, other resonances are difficult to avoid and the crossings will result in prompt beam losses or significant emittance growth. Therefore, the control of the tune shift or spread is very important in the synchrotrons such as the CSNS/RCS. A parameter called the Laslett tune shift

[12] is usually used to evaluate the averaged incoherent tune shift in a synchrotron,

$$\Delta\nu = -\frac{r_p n_t}{2\pi\beta^2\gamma^3\varepsilon B_f}, \quad (7)$$

where $r_p=1.53\times 10^{-18}$ m is the classical radius of a proton, n_t is the accumulated particles in the ring, β and γ are the Lorentz' velocity and energy for the beam, ε is the transverse emittance and B_f is the bunching factor to be discussed in the next subsection. From Eq. (7), one can clearly find that higher injection energy, larger emittance and larger bunching factor are the keys to the reduction in the tune shift in case of accumulating a large number of particles. It is worthwhile noting here that the transverse tune shift is largely influenced by the longitudinal parameter – bunching factor.

2.4 Bunching factor of a beam bunch

To increase the bunching factor is an effective way to control the tune shift, and the acceleration by a dual-harmonic RF system is often applied to enhance the bunching factor. The bunching factor is defined as the ratio of the average current to the peak current of a beam bunch, namely, the ratio of the bunch length to the wavelength of periodic bunches. The bunching factor can also be expressed by [13]

$$B_f = F/(2\pi\hat{H}), \quad (8)$$

where the potential shape is defined by

$$\begin{aligned} \hat{H} = & \cos\phi_{\max} - \cos\phi_2 + (\phi_{\max} - \phi_2)\sin\phi_s \\ & - \frac{\delta}{2}[\cos(2\phi_{\max} + \theta) - \cos(2\phi_2 + \theta)] \\ & - \delta(\phi_{\max} - \phi_2)\sin(2\phi_2 + \theta) \end{aligned} \quad (9)$$

in which, ϕ_{\max} is the extremity of the bucket, and the relative momentum spread F defines the potential area in the case of dual-harmonic. It can be simply extended from the single harmonic form,

$$F(\phi_1, \phi_2) = f(\phi_1, \phi_2) - \frac{\delta}{4}f(2\phi_1 + \theta, 2\phi_2 + \theta), \quad (10)$$

where the single harmonic form is

$$\begin{aligned} f(\phi_1, \phi_2) = & \sin\phi_2 - \sin\phi_1 \\ & - \frac{1}{2}(\phi_1 - \phi_2)(\cos\phi_1 + \cos\phi_2). \end{aligned} \quad (11)$$

3 Dual-harmonic acceleration design for CSNS-II

As discussed above, the aim of dual-harmonic acceleration is to reduce the transverse tune shift in the low energy stage by increasing the bunching factor. The basic parameters at CSNS-II are given in Table 2.

3.1 RF voltage patterns

As described in Sec. 2.1, the RF voltage pattern has two major functions: accelerating the beam and manipulating the beam distribution. As the tune shift due to the space charge effect is very important mainly at low energy, all kinds of measures including a dual-harmonic RF system have been considered to reduce the tune shift. At CSNS-II, three H4 cavities are planned to compose a dual-harmonic RF system together with the eight H2 cavities installed at CSNS-I. With a single harmonic RF system, the tune shift reaches the maximum at about 2 ms in the RCS, when the transverse beam loss or emittance growth is at the most critical moment. With a dual-harmonic RF system, we have the possibility to produce a shallow and flat tune shift curve. The preliminary design shows that the maximum tune shift can be decreased from -0.29 with the H2 cavities alone to -0.18 with the dual-harmonic RF system. The three H4 cavities are turned on only in the initial 7 ms and will be turned off later. The RF voltage patterns for the H2 and H4 cavities are shown in Fig. 3, and the tune shift curves are shown in Fig. 4. The tune shift should keep monotonically increasing after 2 ms to avoid beam loss at higher energy. The required peak voltage for the H4 cavities in total is 50.4 kV, which happens at about 3 ms. This is less than the maximum voltage supplied by three ferrite-loaded cavities having similar design features as the H2 cavities.

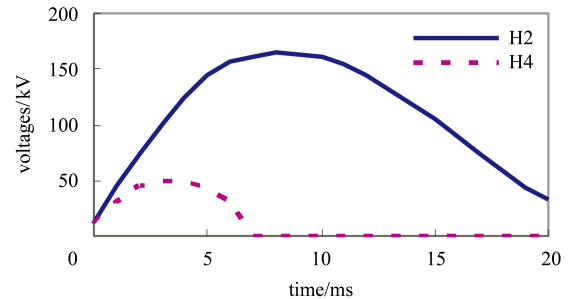


Fig. 3. The RF voltage patterns for the H2 and H4 cavities in total at CSNS-II.

The parameters δ and θ which appeared in Eq. (1) and other formulae are crucial in designing the dual-harmonic RF system. The optimization has been carried out to obtain a large bunching factor and a flattened beam distribution along the beam bunch. Because the maximum tune shift is associated with the maximum line charge density along the bunch, the latter is used for the optimization of the parameter setting. Fig. 4 shows the line charge density with different δ , where the parameter θ is optimized to obtain two equal peak heights.

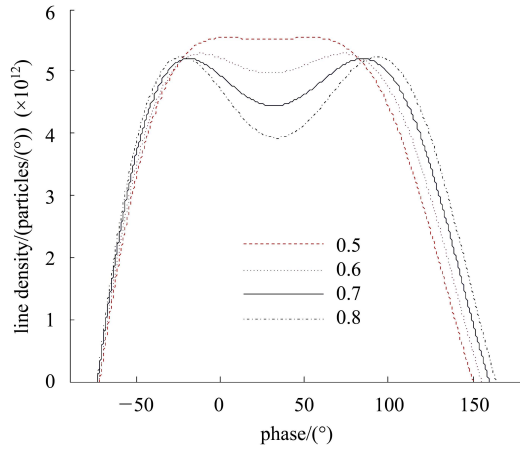


Fig. 4. Line charge density along the beam bunch at 1 ms at CSNS-II.

The parameter δ is determined not only by the optimization of the line charge density but also by the available H4 voltage that has a design limit of 65 kV with three H4 cavities. With increasing H2 voltage along with the time, the maximum applicable δ has to be lowered. Fortunately, the space charge effect also becomes weaker with increasing beam energy. The decrease in δ with time is acceptable, thus a design

to monotonically decrease δ to zero at 7 ms can save the cost of the H4 RF system (see Fig. 5).

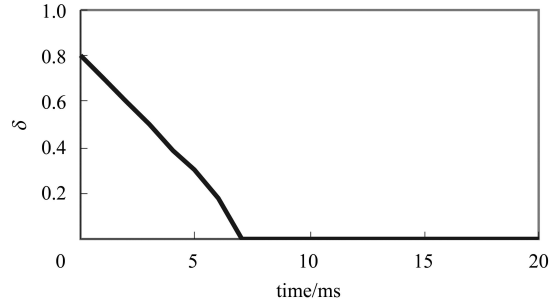


Fig. 5. Pattern of the parameter δ at CSNS-II.

3.2 More details of the design and discussions

The basic longitudinal parameters have been calculated together with the optimization of dual-harmonic RF parameters at discrete moments with a time interval of 1 ms. Suppose the beam loss is 5% during the acceleration cycle, 1.64×10^{13} particles per pulse are used in the calculations. Longitudinal space charge force will shrink the bucket size, so it is also included in the calculations. The main parameters are listed in Table 2.

Table 2. Parameters of dual-harmonic acceleration at CSNS-II.

T/ms	E/GeV	Frf/MHz	$\delta/(\text{°})$	$\phi_s/(\text{°})$	$\theta/(\text{°})$	η_{sc}	$\phi_1/(\text{°})$	$\phi_2/(\text{°})$	V_1/kV	V_2/kV	$Q_s/10^{-3}$	B_f	$\Delta\nu$	$(\Delta p/p)/10^{-3}$	A/eVs
0	0.13	1.26	0.8	0.0	0.0	0.27	-146.2	146.2	12.8	10.2	3.5	0.61	-0.16	3.77	1.00
1	0.14	1.28	0.7	32.2	-51.9	0.23	-73.1	160.1	45.2	31.7	5.9	0.50	-0.18	4.55	1.00
2	0.15	1.34	0.6	39.5	-62.0	0.22	-56.0	159.9	74.1	44.4	6.7	0.47	-0.18	4.59	1.00
3	0.18	1.44	0.5	42.7	-64.1	0.23	-45.3	155.2	100.9	50.4	6.8	0.44	-0.17	4.48	1.00
4	0.22	1.56	0.39	41.1	-61.7	0.22	-36.0	146.9	124.5	48.6	6.7	0.38	-0.17	4.51	1.00
5	0.28	1.68	0.3	40.3	-60.4	0.23	-28.0	138.7	143.5	43.1	6.2	0.32	-0.17	4.54	1.00
6	0.36	1.81	0.18	38.8	-58.3	0.23	-20.8	126.7	157.3	28.3	5.5	0.27	-0.17	4.67	1.00
7	0.44	1.93	0	37.4	0.0	0.22	-14.4	111.5	161.7	0.0	4.8	0.22	-0.17	4.91	1.00
8	0.55	2.04	0	39.7	0.0	0.24	-9.4	110.5	164.2	0.0	4.0	0.21	-0.14	4.55	1.00
9	0.66	2.13	0	41.8	0.0	0.25	-5.0	109.7	163.5	0.0	3.4	0.20	-0.13	4.24	1.00
10	0.78	2.20	0	43.6	0.0	0.27	-1.1	109.0	159.9	0.0	2.8	0.19	-0.11	3.97	1.00
11	0.90	2.26	0	45.1	0.0	0.29	2.1	108.4	153.7	0.0	2.4	0.19	-0.10	3.73	1.00
12	1.02	2.31	0	46.3	0.0	0.31	4.6	107.9	145.0	0.0	2.0	0.18	-0.08	3.53	1.00
15	1.35	2.40	0	47.6	0.0	0.37	7.2	107.4	105.7	0.0	1.2	0.18	-0.06	3.00	1.00
17	1.51	2.43	0	42.8	0.0	0.40	0.5	100.9	73.8	0.0	0.9	0.18	-0.05	2.73	1.00
19	1.59	2.44	0	22.9	0.0	0.43	-24.6	77.6	44.3	0.0	0.8	0.19	-0.05	2.54	1.00
20	1.60	2.45	0	0.0	0.0	0.44	-53.5	53.5	33.6	0.0	0.7	0.20	-0.04	2.42	1.00

Figure 6 shows the bunch shape and the potential curve at 1 ms. Another important parameter – the bunching factor is shown in Fig. 7. From Fig. 8, one can find that the tune shift degenerates just after the injection even with a dual-harmonic RF acceleration.

This can be explained by the facts that the bucket length shrinks with the rapidly changing synchronous phase ϕ_s but the beam energy changes slowly during the period.

In addition, a dual-harmonic system with two H4

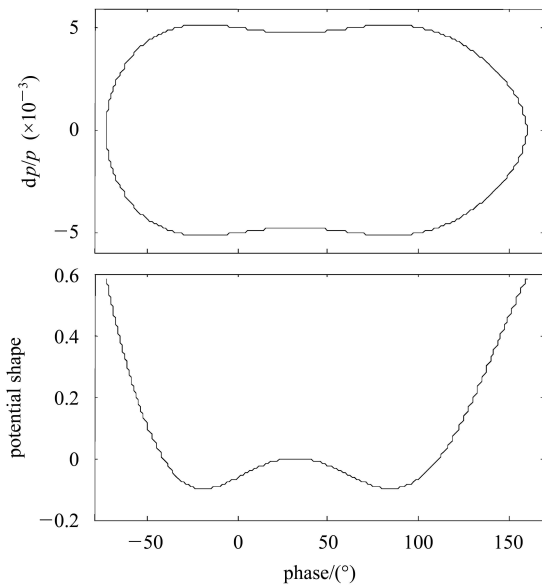


Fig. 6. Bunch shape (upper) and potential curve (lower) at 1 ms at CSNS-II (bucket filling factor is 0.89).

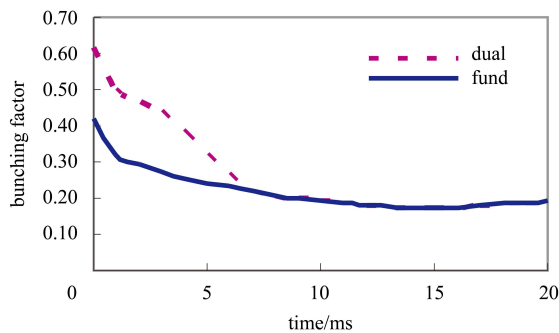


Fig. 7. Bunching factors with dual-harmonic and single harmonic RF systems at CSNS-II.

cavities has also been studied. The enhancement of the bunching factor is modestly worse than with three

H4 cavities, but it is still acceptable if the budget for the upgrading is limited.

In order to obtain more detailed results with the dual-harmonic acceleration, macroparticle simulations using the ORBIT are underway.

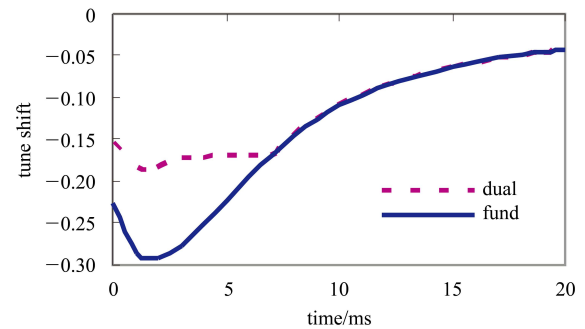


Fig. 8. Tune shift of fundamental acceleration and dual-harmonic acceleration for CSNS-II.

4 Conclusions

A dual-harmonic RF system is proposed for the CSNS upgrading by adding three H4 cavities to the original eight H2 cavities. This study shows that the bunching factor increases significantly if one applies the H4 cavities during the initial 7 ms. The maximum tune shift can be increased from -0.29 with H2 cavities alone to -0.18 with the dual-harmonic RF system. Therefore, the total beam loss rate at CSNS-II is expected to be lower than that at CSNS-I, even with more accumulated particles.

The authors wish to thank the Ring RF Group and the Accelerator Physics Group of the CSNS team for useful discussions.

References

- WEI J, CHEN H S, CHEN Y W et al. Nucl. Instrum. Methods Phys. Res. A, 2009, **600**: 10–13
- CSNS Accelerator Team. Conceptual Design on Chinese Spallation Neutron Source-Accelerators, 2004. IHEP-CSNS-Report/2004-01E (in Chinese)
- Baillod J M, Magnani L, Nassibian G et al. IEEE Trans. Nucl. Sci., 1983, **30**: 3499–3501
- Brennan J M, Roser T. Proc. of PAC1999. New York, 1999. 614–616
- Middendorf M E, Brumwell F R, Dooling J C et al. Proc. of PAC2007. Albuquerque, New Mexico, 2007. 2233–2235
- Seville A, Gardner I, Thomason J et al. Proc. of EPAC2008. Genoa, 2008. 349–351
- Tamura F, Yamamoto M, Yoshii M et al. Phys. Rev. ST Accel. Beams, 2009, **12**: 041001–041009
- Prior C. Studies of Dual Harmonic Acceleration in ISIS. ICANS XII, RAL Report 94025, 1994. A11
- QIU J, TANG J Y, WANG S et al. HEP & NP, 2007, **31**(10): 942–946 (in Chinese)
- Hofmann A, Pedersen F. IEEE Trans. Nucl. Sci., 1979, **26**: 3526–3528
- Lee S Y. Accelerator Physics. Singapore: World Scientific Publishing Co. Pte. Ltd., 1999. 229–230
- Laslett L J. On Intensity Limitations Imposed by Transverse Space-Charge Effects in Circular Particle Accelerators. Proc. 1963 Summer Sch. BNL, 1963. 324–326
- Duke J P, Rees G H, Trotman J V et al. Dual Harmonic Acceleration. ESS 94-12-R, August 1994